

AN IMPROVED SIGNAL-SELECTIVE DIRECTION FINDING ALGORITHM USING SECOND-ORDER CYCLIC STATISTICS

Wen-Jun Zeng[†], Xi-Lin Li[†], Xian-Da Zhang[†], and Xue Jiang[‡]

[†] Department of Automation, Tsinghua University, Beijing 100084, China

[‡] Beijing Sunnorth Electronic Technology Co., LTD, Beijing 100085, China

ABSTRACT

A new signal-selective direction finding algorithm which exploits the property of the cyclostationarity of incoming signals is proposed. After dimensionality reducing by projecting the observed array data onto the signal subspace, the array manifold matrix is identified by the simultaneous diagonalization structure of the matrix pencil consisting of the cyclic correlation matrix and the cyclic conjugate correlation matrix. Then the direction-of-arrivals (DOAs) are obtained from the phase-differences of the estimated array manifold matrix. Simulation results demonstrate that the proposed algorithm is superior to the cyclic-MUSIC and cyclic-ESPRIT in terms of the root mean squares errors (RMSEs) of the DOA estimates.

Index Terms— Direction finding, signal-selectivity, cyclostationarity, simultaneous diagonalization, matrix pencil.

1. INTRODUCTION

Many communication signals exhibit cyclostationarity (or periodic correlation) due to modulation, sampling, multiplexing, etc [1]. It has been shown that the signals can be automatically classified as the desired or undesired according to their cyclostationarity properties, which is referred to as signal-selectivity [2]. In array signal processing, such signal-selectivity can be exploited to estimate only the direction-of-arrival (DOA) of the signals of interest (SOIs) and suppress the effect of interferences and noise.

Several high resolution signal-selective direction finding methods have been developed [2][3][4]. Most of them are based on subspace analysis. The cyclic-MUSIC algorithm [2][3] uses the cyclic correlation matrix instead of the covariance matrix adopted by the conventional MUSIC method. Based on the shift invariant property of the subspace spanned by the cyclic correlation matrix, the cyclic-ESPRIT algorithm is proposed [3]. However, both cyclic-MUSIC and cyclic-ESPRIT use only one single cyclic correlation matrix. The

This work was supported by the National Natural Science Foundation of China under Grant 60675002, and funded by Basic Research Foundation of Tsinghua National Laboratory for Information Science and Technology (TNList).

extended cyclic MUSIC algorithm exploits both cyclic correlation matrix and cyclic conjugate correlation matrix [5]. Thus the extended cyclic MUSIC outperforms cyclic-MUSIC and cyclic-ESPRIT. However, the extended cyclic MUSIC still needs one-dimensional spectral search.

In this paper, a new direction finding algorithm is proposed. First the observed data are projected onto the signal subspace to obtain the lower-dimensional data. Then we identify the array manifold matrix by solving a simultaneous diagonalization problem, which is solved via gradient descent. Finally the estimations of the DOAs are obtained from the phase-differences of the estimated steering vectors. Since the proposed algorithm utilizes the information of both the cyclic correlation and the cyclic conjugate correlation, it delivers better performance than cyclic-MUSIC and cyclic-ESPRIT. Compared with the extended cyclic MUSIC, the proposed approach can avoid any spectral search procedure.

2. SECOND-ORDER CYCLIC STATISTICS

The cyclic autocorrelation function and the cyclic conjugate autocorrelation function of a signal $x(t)$ are defined as [1][3]

$$R_{xx}^{\alpha}(\tau) = \langle x(t)x^{*}(t - \tau)e^{-j2\pi\alpha t} \rangle_t \quad (1)$$

and

$$R_{xx^{*}}^{\alpha}(\tau) = \langle x(t)x(t - \tau)e^{-j2\pi\alpha t} \rangle_t \quad (2)$$

respectively, where $\langle \cdot \rangle_t$ denotes the infinite-time average, $j = \sqrt{-1}$ is the imaginary unit, and the superscript $*$ denotes the complex conjugate. α is referred to as cycle frequency. $x(t)$ is said to be cyclostationary if $R_{xx}^{\alpha}(\tau)$ or $R_{xx^{*}}^{\alpha}(\tau)$ does not vanish at cycle frequency α for some time lag parameter τ . The cyclic cross-correlation function of two signals $x_1(t)$ and $x_2(t)$ are defined as

$$R_{x_1x_2}^{\alpha}(\tau) = \langle x_1(t)x_2^{*}(t - \tau)e^{-j2\pi\alpha t} \rangle_t. \quad (3)$$

If $R_{x_1x_2}^{\alpha}(\tau) = 0$ at some cycle frequency α for all time lag τ , then $x_1(t)$ and $x_2(t)$ are cyclically uncorrelated.

For a given a vector $\mathbf{x}(t) = [x_1(t), \dots, x_M(t)]^T$ of cyclostationary signals, its cyclic correlation matrix and cyclic conjugate correlation matrix are defined as

$$\mathbf{R}_{\mathbf{xx}}^{\alpha}(\tau) = \langle \mathbf{x}(t)\mathbf{x}^H(t - \tau)e^{-j2\pi\alpha t} \rangle_t \quad (4)$$

and

$$\mathbf{R}_{\mathbf{xx}^*}^\alpha(\tau) = \langle \mathbf{x}(t)\mathbf{x}^T(t-\tau)e^{-j2\pi\alpha t} \rangle_t \quad (5)$$

respectively, where the superscript H denotes the conjugate transpose and T the transpose. Note that both cyclic correlation matrix and cyclic conjugate correlation matrix are generally not Hermitian.

In practice, since the length of the observed signal is finite, the cyclic correlation matrices can be estimated by the finite-time average operator.

3. ARRAY DATA MODEL

Consider K cyclically uncorrelated, narrowband sources emitting plane waves impinging on a uniform linear array (ULA) of M sensors with inter-sensor spacing d . It is assumed that there are K_α ($K_\alpha \leq K$) sources are cyclostationary signals with cycle frequency α , which are referred to as signals of interest (SOIs). The DOAs of the SOIs are θ_k ($k = 1, \dots, K_\alpha$).

By arranging the M observed signals in a vector $\mathbf{x}(t) = [x_1(t), \dots, x_M(t)]^T$, the matrix formulation of the array data can be written as

$$\mathbf{x}(t) = \mathbf{A}\mathbf{s}(t) + \mathbf{i}(t) + \mathbf{v}(t) \quad (6)$$

where the vector $\mathbf{s}(t) = [s_1(t), \dots, s_{K_\alpha}(t)]^T$ only contains the cyclostationary sources with cycle frequency α , $\mathbf{i}(t)$ represents other $K - K_\alpha$ interfering sources, and $\mathbf{v}(t)$ denotes additive noise. The array manifold matrix \mathbf{A} is given by

$$\mathbf{A} = [\mathbf{a}(\theta_1), \dots, \mathbf{a}(\theta_{K_\alpha})] \quad (7)$$

where $\mathbf{a}(\theta_k)$ is the steering vector

$$\mathbf{a}(\theta_k) = \left[1, e^{j2\pi\frac{d}{\lambda}\sin\theta_k}, \dots, e^{j2\pi(M-1)\frac{d}{\lambda}\sin\theta_k} \right]^T \quad (8)$$

with λ denoting the wavelength of the signal.

4. THE PROPOSED ALGORITHM

4.1. Eigen-Structure of The Cyclic Correlation Matrices

Note that the following properties hold true:

- 1) The cyclic correlation matrices of the interfering sources $\mathbf{i}(t)$ and noise $\mathbf{v}(t)$ are zeros, i.e., $\mathbf{R}_{\mathbf{ii}}^\alpha(\tau) = \mathbf{R}_{\mathbf{ii}^*}^\alpha(\tau) = \mathbf{R}_{\mathbf{vv}}^\alpha(\tau) = \mathbf{R}_{\mathbf{vv}^*}^\alpha(\tau) = \mathbf{0}$;
- 2) The cyclic cross-correlations between the SOIs and the interfering sources (or noise) are zeros since they are cyclically uncorrelated.

Based on the above properties, we get

$$\mathbf{R}_{\mathbf{xx}}^\alpha(\tau) = \mathbf{A}\mathbf{R}_{\mathbf{ss}}^\alpha(\tau)\mathbf{A}^H \quad (9)$$

$$\mathbf{R}_{\mathbf{xx}^*}^\alpha(\tau) = \mathbf{A}\mathbf{R}_{\mathbf{ss}^*}^\alpha(\tau)\mathbf{A}^T \quad (10)$$

where $\mathbf{R}_{\mathbf{ss}}^\alpha(\tau)$ and $\mathbf{R}_{\mathbf{ss}^*}^\alpha(\tau)$ are the cyclic correlation matrix and the cyclic conjugate correlation matrix of $\mathbf{s}(t)$. Since the sources are assumed cyclically uncorrelated, $\mathbf{R}_{\mathbf{ss}}^\alpha(\tau)$ and $\mathbf{R}_{\mathbf{ss}^*}^\alpha(\tau)$ are both diagonal, i.e.,

$$\mathbf{R}_{\mathbf{ss}}^\alpha(\tau) = \text{diag} \left\{ R_{s_1 s_1}^\alpha(\tau), \dots, R_{s_{K_\alpha} s_{K_\alpha}}^\alpha(\tau) \right\} \quad (11)$$

$$\mathbf{R}_{\mathbf{ss}^*}^\alpha(\tau) = \text{diag} \left\{ R_{s_1 s_1^*}^\alpha(\tau), \dots, R_{s_{K_\alpha} s_{K_\alpha}^*}^\alpha(\tau) \right\}. \quad (12)$$

Equations (9) and (10) mean that the two matrices $\mathbf{R}_{\mathbf{xx}}^\alpha(\tau)$ and $\mathbf{R}_{\mathbf{xx}^*}^\alpha(\tau)$ span the same range space of \mathbf{A} , i.e.,

$$\text{range}(\mathbf{R}_{\mathbf{xx}}^\alpha(\tau)) = \text{range}(\mathbf{R}_{\mathbf{xx}^*}^\alpha(\tau)) = \text{range}(\mathbf{A}). \quad (13)$$

Therefore we can utilize both $\mathbf{R}_{\mathbf{xx}}^\alpha(\tau)$ and $\mathbf{R}_{\mathbf{xx}^*}^\alpha(\tau)$ to identify the range space of the array manifold matrix \mathbf{A} and estimate the DOA parameters. The cyclic MUSIC algorithm only uses a *single* cyclic correlation matrix ($\mathbf{R}_{\mathbf{xx}}^\alpha(\tau)$ or $\mathbf{R}_{\mathbf{xx}^*}^\alpha(\tau)$). Compared with the single matrix-based cyclic-MUSIC and cyclic-ESPRIT methods [1], exploiting two cyclic correlation matrices can obviously improve the performance.

First, we form a new $M \times 2M$ matrix

$$\mathbf{R}_E^\alpha(\tau) = [\mathbf{R}_{\mathbf{xx}}^\alpha(\tau), \mathbf{R}_{\mathbf{xx}^*}^\alpha(\tau)]. \quad (14)$$

According to (13), $\mathbf{R}_E^\alpha(\tau)$ also spans the same range space of \mathbf{A} , i.e.,

$$\text{range}(\mathbf{R}_E^\alpha(\tau)) = \text{range}(\mathbf{A}). \quad (15)$$

The singular value decomposition (SVD) of $\mathbf{R}_E^\alpha(\tau)$ is given by

$$\mathbf{R}_E^\alpha(\tau) = [\mathbf{U}_s \mathbf{U}_n] \begin{bmatrix} \mathbf{\Sigma}_s & \\ & \mathbf{\Sigma}_n \end{bmatrix} [\mathbf{V}_s \mathbf{V}_n]^H \quad (16)$$

where $\mathbf{\Sigma}_s = \text{diag} \{ \sigma_1, \dots, \sigma_{K_\alpha} \}$ is a diagonal matrix containing the K_α principal singular values in descending order and $\mathbf{U}_s \in \mathbb{C}^{M \times K_\alpha}$ contains the corresponding orthonormal left singular vectors. \mathbf{U}_n is the orthonormal complement of \mathbf{U}_s (\mathbf{U}_n is also the left null space of $\mathbf{R}_E^\alpha(\tau)$).

It is clear that \mathbf{A} and \mathbf{U}_s span the same range space, i.e., $\text{range}(\mathbf{A}) = \text{range}(\mathbf{U}_s)$, which indicates that there exists a $K_\alpha \times K_\alpha$ nonsingular matrix \mathbf{W} satisfying

$$\mathbf{A} = \mathbf{U}_s \mathbf{W}. \quad (17)$$

Since the estimation of signal subspace $\hat{\mathbf{U}}_s$ can be calculated by the SVD of $\hat{\mathbf{R}}_E^\alpha(\tau)$, the estimation of array manifold matrix $\hat{\mathbf{A}}$ can be obtained if we find the matrix \mathbf{W} . In the following section, we will introduce a method for identifying \mathbf{W} . By exploiting $\mathbf{U}_s^H \mathbf{U}_s = \mathbf{I}$, (17) can also be written as

$$\mathbf{U}_s^H \mathbf{A} = \mathbf{W}. \quad (18)$$

4.2. Identification of \mathbf{W}

The signal subspace spanned by the columns of \mathbf{U}_s is also referred to as principal components. Project the observed data onto the signal subspace, then a lower-dimensional vector

$$\mathbf{y}(t) = \mathbf{U}_s^H \mathbf{x}(t) \in \mathbb{C}^{K_\alpha} \quad (19)$$

is obtained. It is easy to verify that the cyclic correlation matrix and the cyclic conjugate correlation matrix of $\mathbf{y}(t)$ can be expressed as

$$\begin{cases} \mathbf{R}_{\mathbf{y}\mathbf{y}}^\alpha(\tau) = \mathbf{U}_s^H \mathbf{R}_{\mathbf{x}\mathbf{x}}^\alpha(\tau) \mathbf{U}_s \\ \mathbf{R}_{\mathbf{y}\mathbf{y}^*}^\alpha(\tau) = \mathbf{U}_s^H \mathbf{R}_{\mathbf{x}\mathbf{x}^*}^\alpha(\tau) \mathbf{U}_s^* \end{cases} \quad (20)$$

Substituting (9) and (10) into (20) leads to

$$\begin{cases} \mathbf{R}_{\mathbf{y}\mathbf{y}}^\alpha(\tau) = \mathbf{U}_s^H \mathbf{A} \mathbf{R}_{\mathbf{s}\mathbf{s}}^\alpha(\tau) \mathbf{A}^H \mathbf{U}_s \\ \mathbf{R}_{\mathbf{y}\mathbf{y}^*}^\alpha(\tau) = \mathbf{U}_s^H \mathbf{A} \mathbf{R}_{\mathbf{s}\mathbf{s}^*}^\alpha(\tau) \mathbf{A}^T \mathbf{U}_s^* \end{cases} \quad (21)$$

According to (18), (21) can be expressed as

$$\mathbf{R}_{\mathbf{y}\mathbf{y}}^\alpha(\tau) = \mathbf{W} \mathbf{R}_{\mathbf{s}\mathbf{s}}^\alpha(\tau) \mathbf{W}^H \quad (22)$$

$$\mathbf{R}_{\mathbf{y}\mathbf{y}^*}^\alpha(\tau) = \mathbf{W} \mathbf{R}_{\mathbf{s}\mathbf{s}^*}^\alpha(\tau) \mathbf{W}^T. \quad (23)$$

Equations (22) and (23) mean that the matrix pencil, denoted as $\{\mathbf{R}_{\mathbf{y}\mathbf{y}}^\alpha(\tau), \mathbf{R}_{\mathbf{y}\mathbf{y}^*}^\alpha(\tau)\}$, has the simultaneous diagonalization structure. However, there are two reasons causing that such simultaneous diagonalization problem can not be solved by the generalized eigenvalue decomposition (GEVD) of the matrix pencil $\{\mathbf{R}_{\mathbf{y}\mathbf{y}}^\alpha(\tau), \mathbf{R}_{\mathbf{y}\mathbf{y}^*}^\alpha(\tau)\}$:

- 1) $\mathbf{R}_{\mathbf{y}\mathbf{y}}^\alpha(\tau)$ and $\mathbf{R}_{\mathbf{y}\mathbf{y}^*}^\alpha(\tau)$ are not Hermitian;
- 2) In (22) it is the conjugate transpose term \mathbf{W}^H , whereas in (23) it appears the transpose term \mathbf{W}^T . Therefore it is a bit different from the conventional joint diagonalization problem.

Moreover, this problem has no closed-form solution. In fact, the single equality (22) yields

$$\mathbf{R}_{\mathbf{y}\mathbf{y}}^\alpha(\tau) + \mathbf{R}_{\mathbf{y}\mathbf{y}}^\alpha(\tau)^H = \mathbf{W} (\mathbf{R}_{\mathbf{s}\mathbf{s}}^\alpha(\tau) + \mathbf{R}_{\mathbf{s}\mathbf{s}}^\alpha(\tau)^*) \mathbf{W}^H \quad (24)$$

$$\mathbf{j} (\mathbf{R}_{\mathbf{y}\mathbf{y}}^\alpha(\tau) - \mathbf{R}_{\mathbf{y}\mathbf{y}}^\alpha(\tau)^H) = \mathbf{W} (\mathbf{j} \mathbf{R}_{\mathbf{s}\mathbf{s}}^\alpha(\tau) - \mathbf{j} \mathbf{R}_{\mathbf{s}\mathbf{s}}^\alpha(\tau)^*) \mathbf{W}^H. \quad (25)$$

Clearly \mathbf{W} is a joint diagonalizer of the Hermitian matrix pencil $\{\mathbf{R}_{\mathbf{y}\mathbf{y}}^\alpha(\tau) + \mathbf{R}_{\mathbf{y}\mathbf{y}}^\alpha(\tau)^H, \mathbf{j} (\mathbf{R}_{\mathbf{y}\mathbf{y}}^\alpha(\tau) - \mathbf{R}_{\mathbf{y}\mathbf{y}}^\alpha(\tau)^H)\}$, and \mathbf{W} can be obtained by the GEVD of the Hermitian matrix pencil. Nevertheless, such \mathbf{W} does not necessarily *exactly* diagonalizes $\mathbf{R}_{\mathbf{y}\mathbf{y}^*}^\alpha(\tau)$ with the form of (23). Thus it can be viewed as an *approximate* joint diagonalization problem and an iterative algorithm can be designed to find \mathbf{W} .

Denote the inverse of \mathbf{W} with $\mathbf{Z} = \mathbf{W}^{-1}$, then we can find the joint diagonalizer \mathbf{Z} by minimizing the cost function

$$J(\mathbf{Z}) = \|\text{off}(\mathbf{Z} \mathbf{R}_{\mathbf{y}\mathbf{y}}^\alpha(\tau) \mathbf{Z}^H)\|_F^2 + \|\text{off}(\mathbf{Z} \mathbf{R}_{\mathbf{y}\mathbf{y}^*}^\alpha(\tau) \mathbf{Z}^T)\|_F^2 - \log |\det(\mathbf{Z})| \quad (26)$$

where $\text{off}(\cdot)$ zeros the diagonal elements of a matrix, $\|\cdot\|_F$ is the Frobenius norm, and $\det(\cdot)$ denotes the determinant of a squared matrix. Like the fast approximate joint diagonalization (FAJD) algorithm [6], the first and the second terms of the cost function is the squared off-diagonal error (denoted as

$J_1(\mathbf{Z})$) and the minus logarithmic determinant term can avoid the trivial solution and any singular solutions. This paper considers the gradient-based algorithms minimizing (26).

First solve the optimal scaling problem. For a positive scalar κ ,

$$J(\kappa \mathbf{Z}) = \kappa^4 J_1(\mathbf{Z}) - K_\alpha \log \kappa - \log |\det(\mathbf{Z})| \quad (27)$$

By solving $\frac{dJ(\kappa \mathbf{Z})}{d\kappa} = 0$, the optimal κ is given by

$$\kappa_{\text{opt}} = \sqrt[4]{\frac{K_\alpha}{4J_1(\mathbf{Z})}}. \quad (28)$$

Furthermore, since $\frac{d^2 J(\kappa \mathbf{Z})}{d^2 \kappa} = 12\kappa^2 J_1(\mathbf{Z}) + \frac{N}{\kappa^2} > 0$ for any κ , the κ_{opt} in (28) is the global optimum. Then update \mathbf{W} as $\mathbf{W} \leftarrow \kappa \mathbf{W}$.

Secondly, update \mathbf{W} along the gradient descent direction. Denote

$$\mathbf{B}_1 = \mathbf{Z} \mathbf{R}_{\mathbf{y}\mathbf{y}}^\alpha(\tau) \mathbf{Z}^H, \mathbf{B}_2 = \mathbf{Z} \mathbf{R}_{\mathbf{y}\mathbf{y}^*}^\alpha(\tau) \mathbf{Z}^T. \quad (29)$$

The conjugate-gradient of the cost function can be derived as

$$\begin{aligned} \nabla_{\mathbf{Z}} J(\mathbf{Z}) = & \text{off}(\mathbf{B}_1^H) \mathbf{Z} \mathbf{R}_{\mathbf{y}\mathbf{y}}^\alpha(\tau) + \text{off}(\mathbf{B}_1) \mathbf{Z} \mathbf{R}_{\mathbf{y}\mathbf{y}}^\alpha(\tau)^H \\ & + 2\text{off}(\mathbf{B}_2) \mathbf{Z}^* \mathbf{R}_{\mathbf{y}\mathbf{y}^*}^\alpha(\tau)^* - \frac{1}{2} \mathbf{Z}^{-H}. \end{aligned} \quad (30)$$

Hence the learning rule for \mathbf{Z} is

$$\mathbf{Z} \leftarrow \mathbf{Z} - \mu \nabla_{\mathbf{Z}} J(\mathbf{Z}) \quad (31)$$

where μ is the step size. After finding a joint diagonalizer \mathbf{Z} of the matrix pencil $\{\mathbf{R}_{\mathbf{y}\mathbf{y}}^\alpha(\tau), \mathbf{R}_{\mathbf{y}\mathbf{y}^*}^\alpha(\tau)\}$ based on the gradient descent iteration, we can get the estimate of the nonsingular matrix $\hat{\mathbf{W}} = \mathbf{Z}^{-1}$.

4.3. DOA Estimation

Once we obtain $\hat{\mathbf{W}}$, the array manifold matrix can be estimated using $\hat{\mathbf{A}} = \hat{\mathbf{U}}_s \hat{\mathbf{W}}$, i.e., the estimation of steering vectors $\hat{\mathbf{a}}_k$ ($k = 1, \dots, K_\alpha$) are obtained.

It is easy to extract the DOA parameters from the estimated steering vector $\hat{\mathbf{a}}_k$. According to (8), the phase difference between the p -th element and the $(p+1)$ -th element of $\hat{\mathbf{a}}_k$ equals

$$2\pi \frac{d}{\lambda} \sin \hat{\theta}_k = \text{angle} \left(\frac{\hat{\mathbf{a}}_k(p)}{\hat{\mathbf{a}}_k(p+1)} \right), p = 1, \dots, M-1 \quad (32)$$

where $\hat{\mathbf{a}}_k(p)$ represents the p -th element of $\hat{\mathbf{a}}_k$ and $\text{angle}(\cdot)$ is the phase angle of a complex number. Hence $\hat{\theta}_k$ can be estimated from (32). We can adopt the average of the multiple estimation results as the final estimation for improving the accuracy

$$\hat{\theta}_k = \frac{1}{M-1} \sum_{p=1}^{M-1} \sin^{-1} \left(\frac{\lambda}{2\pi d} \text{angle} \left(\frac{\hat{\mathbf{a}}_k(p)}{\hat{\mathbf{a}}_k(p+1)} \right) \right) \quad (33)$$

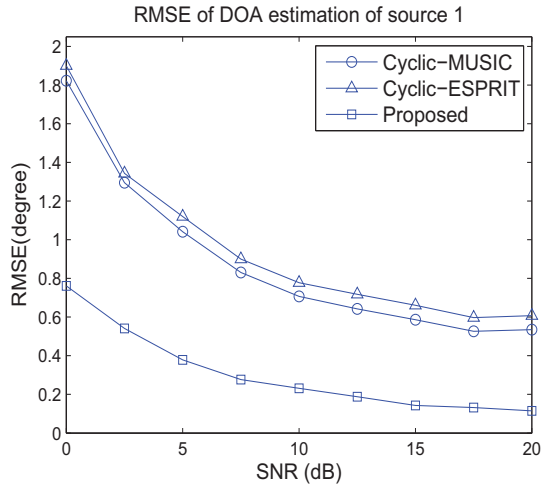


Fig. 1. RMSE of DOA estimates of the 1st SOI versus SNR.

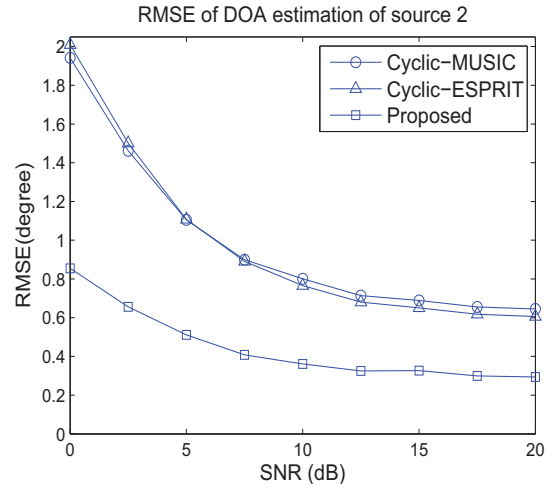


Fig. 2. RMSE of DOA estimates of the 2nd SOI versus SNR.

5. SIMULATION RESULTS

We consider a ULA consisting of $M = 4$ sensors with inter-sensor spacing $d = \lambda/2$. There are three BPSK-modulated sources. Two signals are SOIs with bit rate 4 Mbps. The third signal is considered as interferer, whose bit rate is 3.2 Mbps. Hence the cycle frequencies of the SOIs and the interferer are equal to 4 MHz and 3.2 MHz, respectively. In the simulation experiment, we set the cycle frequency $\alpha = 4$ MHz and the lag parameter $\tau = 0.125 \mu\text{s}$. Therefore the contribution of the interferer signal is theoretically zero in the two cyclic correlation matrices and the cyclic correlation based methods estimate only the DOAs of the SOIs and can suppress the interferer. The observed signals are over-sampled with the sample frequency 32 MHz during 100 μs (i.e., the number of snapshots is equal to 3200).

The DOAs of the two SOIs are $\theta_1 = -10^\circ$, and $\theta_2 = 10^\circ$, respectively. The azimuth of the interferer signal is $\theta_3 = 30^\circ$. The noise is zero-mean and Gaussian white. It is assumed that the three sources have the same power, so the signal-to-noise ratio (SNR) is the same to each signal. The range of SNR is considered to vary from 0 dB to 20 dB.

We compare our algorithm with the cyclic-MUSIC and cyclic-ESPRIT methods. 500 Monte Carlo trials are carried out to evaluate the performance of the three methods. Fig. 1 and 2 illustrate the root mean squared errors (RMSEs) of the estimated DOAs of the first SOI and the second SOI versus SNR, respectively. It is clear that the proposed algorithm outperforms the cyclic-MUSIC as well as the cyclic-ESPRIT.

6. CONCLUSION

A novel direction finding algorithm based on the second-order cyclic statistics is designed. This method exploits the simul-

taneous diagonalization structure of the matrix pencil consisting of both cyclic correlation matrix and cyclic conjugate correlation matrix. An interesting advantage of the proposed algorithm is the capability of selecting the signals with a desired cycle frequency. Numerical simulations are performed to compare the proposed approach with the cyclic-MUSIC and the cyclic-ESPRIT methods. Simulation results validate that the new algorithm achieves biggish improvement in estimation accuracy. However, it requires long enough snapshots to ensure that the contributions of interferers and noise in the cyclic statistics are sufficiently small, which constitutes a drawback of the cyclic statistics based methods.

7. REFERENCES

- [1] W. A. Gardner, A. Napolitano and L. Paura, "Cyclostationarity: Half a century of research," *Signal Processing*, vol. 85, pp. 639-697, 2006.
- [2] S. V. Schell, R. Calabreta, W. A. Gardner and B. G. Agee, "Cyclic MUSIC algorithms for signal-selective direction estimation," in *Proc. IEEE ICASSP*, pp. 2278-2281, 1989.
- [3] W. A. Gardner, "Simplification of MUSIC and ESPRIT by exploitation of cyclostationarity," *Proceedings of the IEEE*, vol. 76, no. 7, pp. 845-847, 1988.
- [4] H. Yan and H. Fan, "Wideband cyclic MUSIC algorithms," *Signal Processing*, vol. 85, pp. 643-649, 2005.
- [5] P. Charge, Y. Wang and J. Saillard, "An extended cyclic MUSIC algorithm," *IEEE Trans. Signal Process.* vol. 51, no. 7, pp. 1695-1701, 2003.
- [6] X.-L. Li and X.-D. Zhang, "Nonorthogonal joint diagonalization free of degenerate solution," *IEEE Trans. Signal Process.* vol. 55, no. 5, pp. 1803-1814, 2007.